NARROWBAND AND WIDEBAND RADIO CHANNEL CHARACTERISTICS IN UNDERGROUND MINING ENVIRONMENTS AT 2.4 GHZ

Chahé NERGUIZIAN [1], Mourad DJADEL [1,2], Charles DESPINS [1] *and* Sofiène AFFÈS [1]

[1] INRS-Télécommunications
800 de la Gauchetière west., suite 6900
Montréal, (Qc) Canada, H5A 1K6
Chahe.Nerguizian@polymtl.ca
Mourad.Djadel@uqat.ca

[2] Bell Nordiq Group Inc.
555 Centrale,
Val d'Or, (Qc) Canada, J9P 1P6
cdespins@promptquebec.com
affes@inrs-telecom.uquebec.ca

Abstract—This paper presents comprehensive experimental results obtained from narrowband and wideband radio channel measurements in an underground mine with narrow veins at 2.4 GHz. From CW measurement data, large-scale distance-power curves and path-loss exponents of the environment are determined. Other relevant parameters such as, mean excess delay, maximum excess delay and rms delay spread are extracted from wideband measurement data. Results show propagation behavior that is specific for these underground environments with rough surfaces.

Index terms—UHF narrowband and wideband measurements, Underground mine, Radio propagation parameters, Multipath time dispersion, Channel path-loss

I. INTRODUCTION

Indoor radio communication has been active areas of research in recent years. Mobile digital radio communication with good performance in underground mines is important in order to improve operational efficiency, workers' safety and remote control of mobile equipment. To be able to achieve this objective, characterization of the radio channel via propagation measurements is essential. Several researchers have reported propagation measurements in and around buildings [1-4]. To the best of our knowledge, few papers consider propagation measurements in an underground mine [5-10], particularly when wideband signals are involved.

The results presented in this paper are based on radio channel measurements made in the CANMET (Canadian Centre for Minerals and Energy Technology) experimental mine in Val d'Or (Québec). A central frequency of 2.4 GHz has been used throughout the measurements in order to have a compatibility with WLAN systems, which may be used for various data, voice and video communication applications.

A standard technique has been used for the narrowband channel measurements. However, due to equipment availability, the wideband channel measurement system has been based on the frequency channel sounding technique [11], [12]. The use of simulation, based on mathematical models, can also be employed [13] to extract the important propagation parameters; however achieving accurate models in such a harsh environment as an underground mine is not easy since the propagation of waves is generally based on multiple reflections, diffraction and diffusion on the rough sidewalls surface.

The objective of this paper is to present the main propagation parameters extracted from experimental results, which can be used for communication applications at 2.4 GHz leading to operational enhancements for the mining industry.

II. MEASUREMENT SYSTEM

A. *Description of the environment*

Measurements were conducted in an underground gallery of a former gold mine, the laboratory mine "CANMET" in Val d'Or, 700 kilometers north of Montréal, Canada. Located at a 40 m underground level, the gallery stretches over a length of 75 meters with a width and height both of approximately 5 meters. Fig. 1 illustrates the plan of the gallery with all its under adjacent galleries.

Due to the curvature of the gallery, the existence of a non line of sight (NLOS) situation is visible. Moreover, the walls are very rough, the floor is not flat and it contains some plaques of water.

0-7803-7822-9/03/$17.00 © 2003 IEEE.

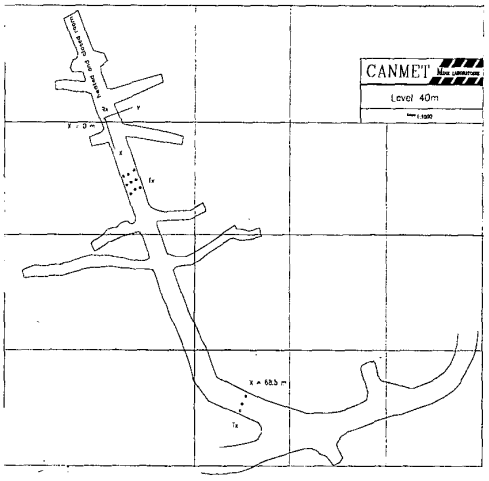

Figure 1. Map of the underground gallery.

B. Measurement setup and experimental protocol

An RF synthesizer (transmitter) and a spectrum analyzer (receiver) have been used for narrowband measurements [10]. For wideband measurements, a vector network analyzer has performed the transmission and the reception of the RF signal. The complex impulse response of the channel has been obtained using the frequency channel sounding technique. The inverse Fourier transform (IFT) has been applied to the measured complex transfer function of the channel in order to obtain its impulse response. The chosen frequency band was centered at 2.4 GHz with a span of 200 MHz corresponding to a theoretical time resolution of 5 nanoseconds (in practice, due to the use of windowing, the time resolution is estimated to be around 8 nanoseconds). The sweep time of the network analyzer has been decreased to validate the quasi-static assumption of the channel (for small displacement of the mobile antenna, most of the reflectors and scatterers remain the same implying a similarity between impulse response functions at points close in space [14]). Each sweep consisted of 201 complex samples spaced of 1 MHz from each other giving an unambiguous delay time (range resolution) of 1 microsecond, which was far beyond the maximum excess delay for the studied mining environment.

For the narrowband measurements, four sets of measurements were taken, with the transmitter, i.e. the synthesizer and the transmit antenna, placed at a different location for each set. The receiver, consisting of the spectrum analyzer, the PC and the receive antenna, was moved to a new position for each power measurement. The position of the transmitter for the four sets was (x=8m, y=1.5m) for TX1, (x=25m, y=0.5m) for TX2, (x=39m, y=0.5m) for TX3 and (x=56m, y=0.5m) for TX4 with respect to the predefined referential (x=0, y=0) of Fig.1. As for the mobile receiver RX, it covered the entire underground gallery (situations with LOS and with NLOS) by varying its position by 1 meter widthwise (3 positions distant of 1 meter for the gallery width of 5 meters) and 2 meters lengthwise (35 positions distant of 2 meters for the gallery length of 70 meters). Some other extra intermediate positions have also been used for the NLOS cases giving a total of 117 location measurements for each transmitter location.

For the wideband measurements [15], the network analyzer and the PC were stationed with the receive antenna and the other receiver components at the predefined referential (Fig.1). The equipments were tested for flat response in the measurement band and calibrated in the presence of the RF cable [16]. The transmit antenna and the other transmitter components were moved to different locations within the underground gallery by varying their position by 0.5 meter widthwise (6 positions distant of 0.5 meter for the gallery width of 5 meters) and 1 meter lengthwise (70 positions distant 1 meter for the gallery length of 70 meters). Some other extra intermediate positions have also been used for the LOS and NLOS cases giving a total of 490 location measurements. For each location, a temporal average has been performed on a set of ten (10) complex transfer function measurements of different observation times (a local spatial average may also be performed). After resolving the ambiguity due to the uncertainty in the phase response [17], the time domain magnitude of the complex impulse response has been obtained, from the measured samples of the frequency domain response, using the inverse Fourier transform (IFT). From the magnitude of the complex impulse response, the mean excess delay (τ_m), the rms delay spread (τ_{rms}), the maximum excess delay (τ_{max}), the relative multipath total power (P), the number of multipath components (N), the power of the first path (P_1) and the arrival time (delay) of the first path (τ_1) of the channel have been computed at all 490 measurement locations by using predefined thresholds of 10, 15, 20 and 26 dB for the multipath noise floor. The first five (5) parameters characterized the time-spread nature of the indoor channel and the last two (2) parameters emphasized the difference between LOS and NLOS situations.

During the narrowband and the wideband measurements, transmit and receive antennas were both mounted on carts at a height of 1.9 meters.

III. Experimental Results

A. Narrowband experimental results and analysis

The total received power P_r, measured at all 117-measurement locations with four different transmitter locations, versus the distance d (consisting of measurement locations situated at both sides of the transmitters) is shown in Fig.2. Using the linear regression fit to the four sets of measurements data, path loss exponent values of the channel have been found to be equal to 2.13, 2.33, 2.15 and 2.17 respectively.

The value of the path loss, for the combined four sets of data, has been determined to be equal to 2.16 with a standard deviation (σ) of 6.13.

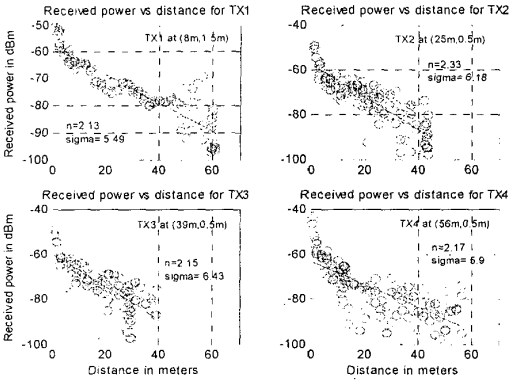

Figure 2. Total received power as a function of distance with four different transmitter locations.

On the other hand, the total received power P_r can provide a means of inferring user location. To visualize the correlation between the received power and the spatial location of a user, a plot of the total received power from each transmitter (TX1, TX2, TX3 and TX4) as a function of the distance along a walk (the walk or the movement of the receiver starting from the predefined reference and terminating at the end of the gallery) is given in Fig.3. Not surprisingly, the signal power at the user or the receiver (RX) is the strongest when the transmitter (TX) is close to it and weakest when it is far away. From the results, it can be seen that the signal level variations, for locations very close to each other, may be as much as 20 dB.

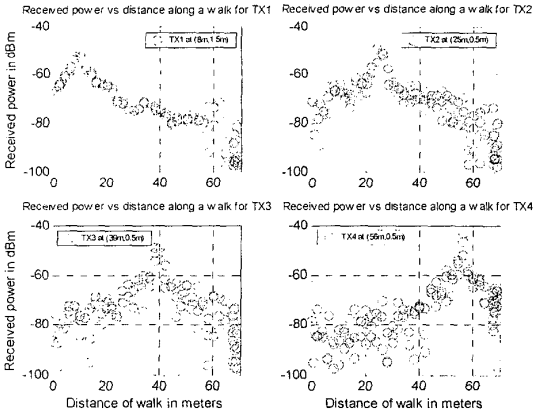

Figure 3. Total received power from four transmitters as a function of distance along a walk in the underground gallery.

B. Wideband experimental results and analysis

1) Typical frequency response function of the channel H(f): The complex transfer function was obtained at all 490 measurement locations. For each location, a temporal average has been performed on a set of ten measurements of different observation times. The magnitude (dB) and phase (degrees) of a typical frequency response as measured by the network analyzer are presented in Fig.4. Dips or notches in the magnitude curve, illustrate the frequency selective nature of fading in the indoor gallery channel. The phase is mostly linear except for large phase shifts, which occur when deep fades are present.

2) Typical magnitude of the complex impulse response of the channel $|h(\tau)|$: The time domain magnitude of the complex impulse response has been obtained from the measured samples of the frequency domain response using the inverse Fourier transform (IFT). The magnitude of the computed time domain response (complex impulse response) for a specific TX-RX separation is given in Fig.5. A dominant LOS component and many multipath components with various propagation delays can be clearly seen.

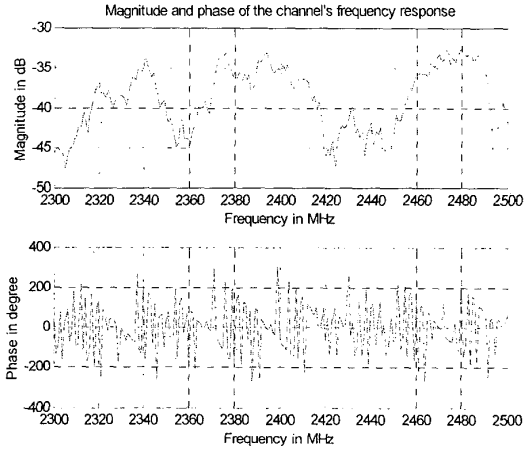

Figure 4. Magnitude (dB) and phase (degrees) of a typical measured frequency response.

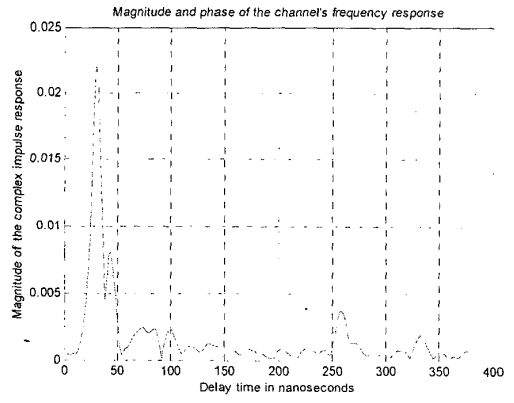

Figure 5. Magnitude of the computed time domain response (magnitude of the complex impulse response) for a specific TX-RX separation.

3) Wideband relevant parameters of the channel: The mean excess delay τ_m, the rms delay spread τ_{rms}, the maximum excess delay τ_{max} (delay span between the first crossing above the predefined threshold level and the last crossing below it), the relative multipath total power P and

the number of multipath components N were computed and their statistics were extracted, from the magnitude of the complex impulse response of the channel, at all 490 measurement locations by using predefined thresholds for the multipath noise floor.

Fig.6 shows a plot of τ_{rms} against distance for a threshold value of 20 dB. The threshold is referenced to the peak line-of-sight (LOS) component of the magnitude of the complex impulse response of the channel. It has to be noted that the magnitude of the complex impulse response in dB corresponds to the power delay profile (PDP) in dB, i.e.$20*\log(|h(\tau)|)=10*\log(PDP)$.

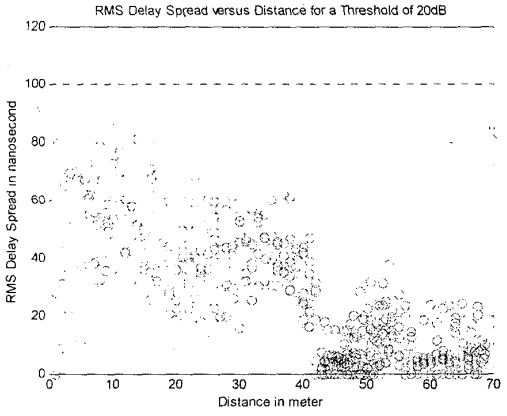

Figure 6. Rms delay spread as a function of distance, for a threshold value of 20 dB.

For in-building environments, in which the transmitter and the receiver are confined to a closed structure, the reported τ_{rms}–distance profile in [11] and [18] follows a dual-slope relation in which τ_{rms} increases with distance and decreases again after a certain separation between TX and RX.

For the considered underground gallery, the profile seen in Fig.6 is not monotonically increasing as may be expected. Results thus show propagation behavior that is specific for these underground environments. This is likely due to the rough sidewalls surface scattering (a difference of 25cm between the maximum and minimum surface variations). On Moreover, τ_{rms} is a location-dependent parameter and its value depends on x and y. Hence, for two locations having the same separation distance between TX and RX, τ_{rms} exhibits two different values even in the absence of the shadowing effect.

On the other hand, the plot in Fig.6 shows that, for a transmitter located after the point of curvature of the underground gallery, τ_{rms} has a relatively small value compared to the cases where the transmitter is closer to the receiver. This is probably due to the high path loss of the channel (TX located at the far region of the RX with NLOS conditions), which eliminates multipath components arriving with longer delays and reduces the number of detectable paths implying a decrease of the τ_{rms} value.

In Fig.7, the cumulative distribution function of τ_{rms} is plotted for different threshold values (10, 15, 20 and 26 dB).

It can be seen that 50% of all locations, in the investigated underground gallery, are equal to or less than 6, 12, 24 and 32 nanoseconds for threshold values of 10, 15, 20 and 26 dB respectively.

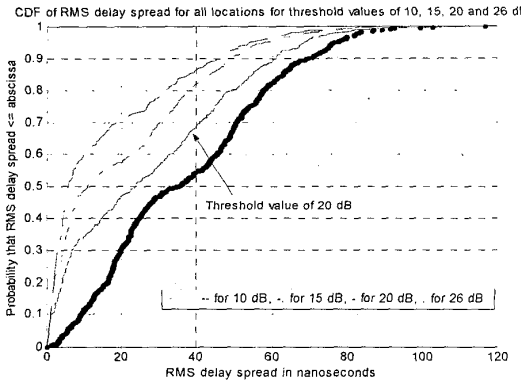

Figure 7. Cumulative Distribution Function of trms for four different threshold values (10, 15, 20 and 26 dB).

The mean, the standard deviation and the maximum of τ_m, τ_{rms} and τ_{max}, for a threshold value of 20 dB, have been computed from the time domain responses and summarized in Table 1.

TABLE 1. MEAN, STANDARD DEVIATION AND MAXIMUM OF τ_m, τ_{rms} AND τ_{max} FOR A THRESHOLD VALUE OF 20 DECIBEL.

All locations	*mean*	*std*	*max*
τ_m (nsec)	16.5	20	127
τ_{rms} (nsec)	27.5	23.5	116
τ_{max} (nsec)	152	119.5	388

Plots of relative multipath total power P and number of multipath components N, for a threshold value of 20 dB, against distance are shown in Fig.8 and Fig.9 respectively.

Fig.8 shows two distinct areas of propagation separated by the point of curvature of the underground gallery as reported in [10]. For the region starting from the predefined referential until the point of curvature (mostly LOS propagation), the decrease of the relative multipath total power with distance is less severe than the one obtained from the critical point until the end of the gallery.

On the other hand, the τ_{rms}-distance and N-distance profiles seen in Fig.6 and Fig.9 exhibit similar variations confirming that, for the far region, multipath components arriving with longer delays and subjected to a high path loss are not detectable. Moreover, it has been noticed that the application of the threshold value, to screen multipath components, affected the value of N significantly. The mean value, the standard deviation and the maximum value of N for all locations, using a threshold of 20 dB, have been found to be equal to 7, 5 and 25 respectively.

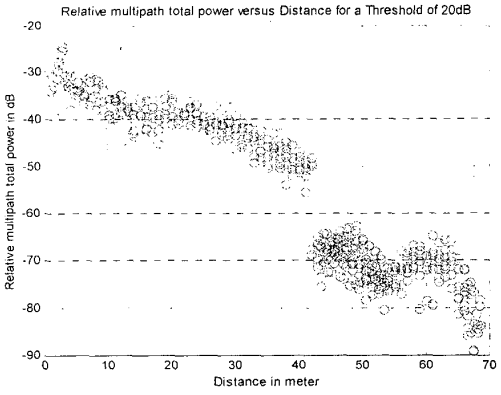

Figure 8. Relative multipath total power as a function of distance, for a threshold value of 20 dB.

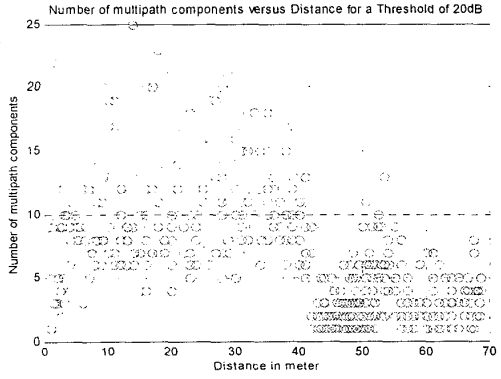

Figure 9. Number of multipath components as a function of distance, for a threshold value of 20 dB.

IV. Conclusions

The results of the wideband measurements show that the τ_{rms}-distance profile is specific to the studied underground gallery. Due to the rough sidewalls surface, the rms delay spread is found to be function of the two-dimensional location of the user. Furthermore, for the majority of locations (90% of the cases), the τ_{rms} value is less than 60 nanoseconds.

On the other hand, the coherence bandwidth, computed from the mean value of τ_{rms}, is approximately equal to 7 MHz (inverse of five times the τ_{rms} mean value). Hence, when transmitting a signal having a bandwidth larger than 7 MHz through the underground gallery, frequency-selective effects will be observed in the channel.

Finally, it has been noted that, for the studied underground gallery with low human activity, the impulse response of the channel is reproducible and respects the uniqueness property (the impulse response of the channel in one location is relatively different from the one in another location).

Acknowledgment

The authors wish to thank M. Ahmed Belyazid for his precious help in the measurements campaign. The financial support of Bell Nordiq Group Inc. is also acknowledged.

References

[1] H. Hashemi, " The Indoor Radio Propagation Channel ", Proceedings of IEEE, Vol. 81, No. 7, pp. 941-967, July 1993

[2] T.S. Rappaport, "Characterization of UHF Multipath Radio Channels in Factory Buildings ", IEEE Transactions on Antennas and Propagation, Vol. 37, No. 8, pp. 1058-1069, August 1989.

[3] D.M.J. Devasirvatham, " A Comparison of Time Delay Spread and Signal Level Measurements within two Dissimilar Office Buildings ", IEEE Transactions on Antennas and Propagation, Vol. 35, No 3, pp. 319-324, march 1987

[4] L. Talbi and G.Y. Delisle, " Experimental Characterization of EHF Multipath Indoor Radio Channels ", IEEE Journal on Selected Areas in Communications, Vol. 14, No. 3, April 1996.

[5] M. Hämäläinen, J. Talvitie, V. Hovinen and P. Leppänen, " Wideband Radio Channel Measurement in a Mine ", Proceedings of the IEEE 5th International Symposium on Spread Spectrum Techniques and Applications, Vol. 2, pp. 522-526, 1998

[6] M. Liénard and P. Degauque, " Natural Wave Propagation in Mine Environments ", IEEE Transactions on Antennas and Propagation, Vol. 48, No 9, pp. 1326-1339, September 2000.

[7] . P. Zhang, G. X. Zheng and J. H. Sheng, " Radio Propagation at 900 MHz in Underground Coal Mines ", IEEE Transactions on Antennas and Propagation, Vol. 49, No. 5, pp. 757-762, May 2001

[8] M. Liénard and P. Degauque, " Mobile Telecommunication in Mine: Characterization of Radio Channel ", 8th Mediterranean Electrotechnical Conference, MELECON 96, Vol. 3, pp. 1663-1665, 1996

[9] B.L.F. Daku, W. Hawkins and A.F. Prugger, " Channel Measurements in Mine Tunnels" , IEEE 55th Vehicular Technology Conference, Vol. 1, pp. 380-383, VTC Spring 2002

[10] M. Djadel, C. Despins and S. Affès, " Narrowband Propagation Characteristics at 2.45 and 18 GHz in Underground Mining Environments " , Proceedings IEEE GLOBECOM 2002, Taipai, Taïwan, November 2002

[11] A.F. AbouRaddy, S.M. Elnoubi and A. El-Shafei, " Wideband Measurements and Modeling of the Indoor Radio Channel at 10 GHz, Parts I and II ", 15th National Radio Science Conference, February 1998

[12] K. Pahlavan and A.H. Levesque, " Wireless Information Networks ", Wiley Edition, 1995.

[13] M. Ndoh and G.Y. Delisle, , " Propagation of Millimetric Waves in Rough Sidewalls Mining Environment ", Vehicular Technology Conference, VTC 2001 spring, Vol. 1, pp. 439-443, Greece, 2001.

[14] Homayoun Hashemi, Michael McGuire, Thomas Vlasschaert et David Tholl, " Measurements and modeling of temporal variations of the indoor radio propagation channel, " IEEE Trans. Veh. Technol., 43 (3), pp. 733-737, August 1994.

[15] G.J.M. Janssen, P.A. Stigter and R. Prasad, " Wideband Indoor Channel Measurements and BEP Analysis of Frequency Selective Multipath Channels at 2.4, 4.75 and 11.5 GHz ", IEEE Transactions on Communications, Vol. 44, pp. 1272-1288, October 1996.

[16] G. Morrison, H. Zaghloul, M. Fattouche, M. Smith and A. McGirr, " Frequency Measurements of the Indoor Channel : System Evaluation and Post Processing using IFDT and Arma Modeling ", IEEE Pacific Rim on Communications, Computers and Signal Processing, May 1991

[17] L. Rusch, C. Prettie, D. Cheung, Q. Li and M. Ho, " Characterization of UWB Propagation from 2 to 8 GHz in a Residential Environment ", Technical paper of UWB technology, Intel Corporation, Intel Research Labs, 2002.

[18] R.J.C. Bultitude at al., " The Dependence of Indoor Radio Channel Multipath Characteristics on Transmit/Receive Ranges ", IEEE JSAC, Vol. 11, No. 7, September 1993.